Article

Not peer-reviewed version

Circuitous Ways of EWS::FLI1: Using Circular RNA ZNF609 to Evade Translational Repression by miR-145 in Ewing's SARCOMA

Aakash Koppula , Ahmed Abdelgawad , Victoria Beringer , Vijay Parashar , Mona Batish *

Posted Date: 1 December 2025

doi: 10.20944/preprints202511.2252.v1

Keywords: Ewing's Sarcoma; EwS; EWS:: FLI1; Circular RNA; circRNA; circZNF609; microRNA; miRNA; miR145

 doi:10.20944/preprints202511.2252.v1

Article

Circuitous Ways of EWS::FLI1: Using Circular RNA ZNF609 to Evade Translational Repression by miR-145 in Ewing's SARCOMA

Aakash Koppula [1,2], Ahmed Abdelgawad [1,2], Victoria Beringer [2], Vijay Parashar [1,2] and Mona Batish [1,2,*]

[1] Department of Biological Sciences

[2] Department of Medical and Molecular Sciences, University of Delaware, 15 Innovation way, Newark, DE, 19711, USA

* Correspondence: batish@udel.edu

Abstract

Ewing's sarcoma (EwS) is a pediatric bone and soft tissue cancer driven by the oncogenic fusion protein EWS::FLI1, with no current targeted therapies. Although the role of some of the non-coding RNAs (ncRNAs) including microRNAs and long non coding RNAs have been explored in EwS, no work is reported on presence and role of newly appreciated class of regulatory RNAs called circular RNAs (circRNA). Our work here reports the first identification and functional characterization of the role of circRNA circZNF609 in EwS. Here we identify and characterize circZNF609, a circRNA expressed in an EWS::FLI1-dependent manner, which promotes EwS cell proliferation, metastasis, and inhibits apoptosis. Mechanistically, circZNF609 acts as a sponge for miR-145-5p, preventing miRNA-mediated translational repression of EWS::FLI1, thereby sustaining oncogenic signaling. Inhibition of miR-145-5p partially rescues the effects of circZNF609 knockdown, confirming this regulatory axis. These findings reveal circZNF609 as a novel post-transcriptional regulator of EWS::FLI1 and suggest its potential as a therapeutic target in EwS.

Keywords: Ewing's Sarcoma; EwS; EWS:: FLI1; Circular RNA; circRNA; circZNF609; microRNA; miRNA; miR145

1. Introduction

Ewing's sarcoma (EwS) is a bone and soft tissue cancer in children, with an incidence of approximately 2–4 cases per million, and is associated with a very high mortality rate upon metastasis (Grünewald et al., 2018). The molecular cause of EwS is a chromosomal rearrangement between the EWSR1 gene on chromosome 22 and members of the ETS gene family (most commonly FLI1, in 90% of cases) on chromosome 11, resulting in the formation of the aberrant oncogenic fusion protein EWS::FLI1. EWS::FLI1 is known to function as an enhancer, transcription factor, and splicing mediator to initiate tumorigenic changes; however, the precise mechanisms by which this single, highly disordered oncogenic protein drives tumor progression remain incompletely understood (May et al., 1993a, 1993b). The lack of structural information and the unstable nature of the fusion protein have made it challenging to develop drugs targeting EWS::FLI1, which would otherwise be an ideal therapeutic target. Although the EWSR1-FLI1 fusion has been recognized as the molecular cause of EwS for over 40 years, no targeted therapies are currently available. As a result, alternative approaches have focused on understanding the interacting partners and downstream effectors of EWS::FLI1, with most work to date emphasizing chromatin regulation (Figuerola-Bou et al., 2025) and epigenetics (Fan et al., 2024) and protein partners (Deng et al., 2022). However, the contribution of non-coding RNAs (ncRNAs) to Ewing's Sarcoma pathogenesis remains poorly understood. Given that EwS cells have a relatively stable genome (Grünewald et al., 2018), it is important to explore non-

 doi:10.20944/preprints202511.2252.v1

genetic regulatory factors that may contribute to EWS::FLI1-mediated transformation, in order to identify novel therapeutic targets.

The majority of the human genome is transcribed into ncRNAs, whose regulatory roles are only beginning to be appreciated (Derrien et al., 2012). Among these, a newly recognized class of ncRNAs, circular RNAs (circRNAs), have been shown to play regulatory roles in various cancers, and their mechanisms of action are an emerging area of research (Kristensen et al., 2019; Li et al., 2018). CircRNAs are covalently closed RNA molecules with no free ends, typically formed by base pairing between repeat regions of long introns flanking exons, leading to back-splicing and the release of a circular molecule. While circRNAs can be derived from exons, introns, or a combination of both, exonic circRNAs are considered the most clinically relevant (Jeck et al., 2013; Memczak et al., 2013). Although circRNAs were discovered about 40 years ago, they were long considered splicing errors until the last decade, when their roles in various physiological processes began to be elucidated (Kristensen et al., 2019). The most studied function of circRNAs is their ability to act as microRNA (miRNA) sponges (Hansen et al., 2013). A growing body of literature has identified functional roles for circRNAs in the progression of many cancers (Kristensen et al., 2019; Li et al., 2018). Reducing their expression or blocking their interactions with targets has led to dramatic changes in cancer progression, suggesting that circRNAs may be promising therapeutic targets (Li et al., 2018; Su et al., 2019). Furthermore, due to their resistance to exonucleases and their enrichment in extracellular vesicles (EVs), circRNAs are promising biomarkers for non-invasive and early diagnosis of many solid tumors (Li et al., 2018). Despite the recognition of multiple critical roles for circRNAs in various cancers, including osteosarcoma (Su et al., 2019), there have been limited studies characterizing circRNAs in EwS cells or in EVs derived from EwS cells. While the roles of miRNAs and long ncRNAs in EwS oncogenesis have been previously studied (Ban et al., 2011; Barrett et al., 2021; McKinsey et al., 2011), the expression and function of circRNAs in EwS remain unexplored. In this study, we focus on circZNF609, a known oncogenic circRNA previously reported in several cancers, including breast cancer and hepatocellular carcinoma (He et al., 2020; Wang et al., 2018). CircZNF609 has also been reported to act as a sponge for miR-145 and other miRNAs in several cancers (Qian et al., 2021; Wang et al., 2018). Here, we report that circZNF609 is expressed in an EWS::FLI1-dependent manner in EwS and acts as a miR-145-5p sponge, thereby preventing miR-145-5p from binding to the 3′ UTR of EWS::FLI1. This relieves miR-145-5p-mediated suppression of EWS::FLI1 and contributes to EwS oncogenesis.

2. Material and Methods

Cell lines and cloning: HEK 293T (CRL-3216, ATCC) cell line was cultured in DMEM (Millipore Sigma, St. Louis, MO, USA, D6429) supplemented with 10% FBS (Millipore Sigma, St. Louis, MO, USA, F2442), penicillin/streptomycin (Millipore Sigma, St. Louis, MO, USA, P4333) and L-glutamine (Millipore Sigma, St. Louis, MO, USA, G7513). A673 inducible cell line was cultured in above mentioned DMEM further supplemented with HEPES and Non-essential amino acids. TC32 cell line was cultured in RPMI media supplemented with 10 % FBS, penicillin/streptomycin and HEPES. Briefly, shRNA targeting the BSJ of circZNF609 was cloned into the pLKO.1-TRC cloning vector (Addgene Plasmid 10878) and transfected into 293T EBNA cells for virus production. Scrambled shRNA sequence was cloned into pLKO.1-TRC cloning vector and was used as a negative control. A673 inducible and TC32 cells were transduced with virus, and stable cell lines were selected via puromycin (Gibco, Waltham, MA, USA, A11138-03). All cells were cultured at 37 °C with 5% CO2. For imaging studies, all cells were grown on 0.1% gelatin (Bio-Rad, Hercules, CA, USA, 170-6537) coated coverslips in 100 cm^2 petri dishes until 70-80% confluent before fixing in 4% PFA (Millipore Sigma, St. Louis, MO, USA, F8775) and permeabilizing in 70% ethanol for hybridization.

Probe synthesis and purification: Sets of 45-50 linear oligonucleotide probes, each 20 nucleotides in length, were designed complementary to specific regions of ZNF609 and circZNF609 RNA molecules along with an amino group on their 3′ ends (Biosearch Technologies, Novato, CA, USA) to generate PC and PL probes for the ZNF609. The probes were pooled in equimolar

 doi:10.20944/preprints202511.2252.v1

concentrations and conjugated with Texas Red [TR] (Invitrogen, Waltham, MA, USA, T6134), or Cy5 (GE Healthcare, Chicago, IL, USA, PA25001) fluorophores and purified by high-pressure liquid chromatography as previously described in (Batish and Tyagi, 2019).

In-situ circFISH Hybridization: Coverslips with fixed adherent cells were washed with 2× saline sodium citrate solution (Ambion, Austin, TX, USA, AM9763) containing 20% formamide (Ambion, Austin, TX, USA, AM9342/44) and 2 mM ribonucleoside-vanadyl complex (New England Biolabs, Ipswich, MA, USA, S1402S), then cells were hybridized with probe sets in hybridization buffer containing 25 ng/μL of each probe set. Hybridization was done overnight at 37°C in a moist chamber. On the next day, the coverslips were washed three times and stained with DAPI (Sigma, St. Louis, MO, USA, D9542) and mounted on glass slides for imaging.

Fluorescence imaging and analysis: All images were captured with 100× oil objective using a Nikon TiE Inverted epi Fluorescence microscope equipped with a pixis 1024b camera (Princeton Instruments). The images were obtained using Metamorph imaging software. Z-stack images were captured for each fluorescent wavelength at 2 sec exposures, for a total of 16 stacks, 0.2 mm apart. The compiled z-stack images were analyzed using an in-house designed algorithm with MATLAB software (MathWorks, Natick, MA, USA) that identifies spot-like signals in each image and determines their three-dimensional coordinates, then identifies spots that have a counterpart within a 250-nm distance in the other channel. Spots meeting this criterion are classified as co-localized. Each imaging experiment was performed to obtain at least 100 cells counts. The numbers present average molecules with errors indicating 95% confidence interval. The p-values were obtained using Student's t-test.

qRT-PCR: Total RNA was extracted from cells lysed in Trizol (Sigma, St. Louis, MO, USA, T9424) and equal concentrations of RNA from different cells were used for cDNA synthesis using iScript Reverse Transcription Supermix (Bio-RAD, Hercules, CA, USA, 1708841), and gene expression was analyzed using iTaq Universal SYBR Green Supermix (Bio-RAD, Hercules, CA, USA, 1725124) according to manufacturer's protocol. List of primers is provided in supplementary table S1

Immunofluorescence: For immunofluorescence, the permeabilized A673 and TC32 cells were incubated with blocking buffer followed by overnight incubation at 4 ºC with primary antibodies. The subsequent day, another blocking step was performed followed by incubation with a secondary antibody for 1 hour at room temperature and followed by four to five washes with PBS. For imaging, the cells were mounted with DAPI containing mounting medium and imaged using a 100X oil objective in Nikon TiE inverted fluorescence microscope equipped with a CCD Princeton Pixis 1024b camera. The images were acquired using Metamorph software The corrected total cell fluorescence (CTCF) was calculated using ImageJ(Schneider, Rasband, and Eliceiri 2012) and the following formula was applied: CTCF = integrated density–(area of selected cell × mean fluorescence of background readings) as per (McCloy et al., 2014). List of antibodies is provided in supplementary table S1.

Proliferation assay: Cell proliferation was performed using 3-(4, 5-dimethylthiazol-2-yl)-2, 5-diphenyltetrazolium bromide (MTT) Cell Proliferation kit (Roche, Basel, Switzerland, 11465007001). After harvesting the cells, they were reseeded in 96 wells plate with approximately 5000 cells/well with media and maintained at 37°C c in CO2 incubator for 96 hours. Cells were treated based on the manufacturer's protocol at 0, 24, 48, 72 and 96 hours timepoints using a plate reader.

Annexin V assay: Annexin V/Propidium Iodide staining was done using Annexin V Alexa Fluor 488 and Propidium Iodide kit (Invitrogen, Waltham, MA, V13241). In brief, EwS cells were washed with PBS and harvested. Cells were then resuspended in Annexin V binding buffer and diluted to approximately $1x10^6$ cells. Later, based on manufacturer's protocol the assay was performed in BD Fusion Aria flow-cytometer and analyzed using FlowJo software.

Soft agar colony assay: EwS cells with and without circZNF609-KD were passaged and seeded in a 12-well plate (5000 cells/ well) in a soft agar assembly. The bottom agar layer was 0.5% agar mixed with media and the top layer constituted 0.3% agar mixed with cells and media, the soft agar assembly was further topped with media to prevent drying of agar. Cells were cultured at 37°C for 2

 doi:10.20944/preprints202511.2252.v1

weeks. The wells were then stained with 0.01% crystal violet for 30 mins and destained with dH20. The colonies were counted under a dissection microscope using general protocol (Du et al., 2017).

Polysome fractionation: Ribosomal subunits and polysomes were resolved from A673 WT, A673 EWS::FlI1, A673 circZNF609-KD cell extracts by size-exclusion chromatography according to a published protocol (Yoshikawa et al., 2018). Briefly, cells were grown to 80% confluency before performing lysis. The size exclusion column (SEC) employed for polysome fractionation was Bio SEC-5, 5 µm particles, 2000 Å, 7.8 x 300 mm (Agilent Technologies, Santa Clara, CA, USA, 5190-2541) using a Dionex Ultimate 3,000 uHPLC system (Thermo Fisher Scientific, Waltham, MA, USA). Later, total RNA was extracted from each of the fractions using Trizol extraction. Equal concentrations of RNA from all the cell lines were used to make cDNA using iScript Reverse Transcription Supermix. The obtained cDNA was used as a template to analyze expression of EWS::FLI1 as well as reference genes (GAPDH & B-Actin) using iTaq Universal SYBR Green Supermix (Bio-RAD, Hercules, CA, USA, 1725124).

Western Blotting: Cells were lysed in cold RIPA buffer containing protease inhibitor cocktail for 30 mins. Lysate was centrifuged @ 14000g/4°C for 15 mins. 10ug of total protein was boiled with 2x loading dye and denatured proteins were run on 12% SDS-PAGE gel, following which an overnight wet transfer assembly system was used to transfer the proteins on the gel to a PVDF membrane. The following day, the membrane was washed, blocked and then treated with corresponding antibody overnight at 4°C. Next day, membrane was washed thrice with 1x TBST and incubated with secondary antibody dissolved in 5% blocking buffer for 1 hour at RT. Membrane was later washed with 1x TBST 3-5 times before imaging with SuperSignal™ West Pico PLUS Chemiluminescent Substrate (Thermo Scientific, Waltham, MA, USA, 34580) as per manufacturer's protocol.

Luciferase assay: Cells were cultured in a 12 well plate at around 40-50% confluency after which they were transfected with either psiCHECK2-FLI1 3'UTR F1, psiCHECK2-FLI1 3'UTR F2 or psiCHECK2-empty vector as control using Bio-T transfection reagent (Bioland Scientific LLC) as per manufacturer's protocol. After 24-48 hours lysates were harvested using passive lysis buffer. Later Firefly and Renilla Luciferase readings were taken in a plate reader using the Dual-Luciferase Reagent Assay System (Promega, Madison, WI, USA, E1910) as per the manufacturer's protocol. Firefly luciferase (expressed constitutively) obtained after transfection was used to normalize bioluminescence values attained for Renilla luciferase which was expressed in fusion with the 3'UTR of FLI1. The corrected values were then sequentially normalized to the levels obtained in mock and psiCHECK2-empty vector transfections. Each experiment was repeated in triplicate and Student's t-test was done to obtain p values.

Bioinformatic Prediction and Analyses: Functionally relevant miRNAs targeting FLI1 3' UTR were predicted using TargetScan and miRDB databases. MiRNAs interacting with circZNF609 and FLI1 3'UTR were predicted using miRanda v3.3a, circInteractome/TargetScan and miRDB (Chen and Wang, 2020; Dudekula et al., 2016; McGeary et al., 2019). Further comparison of the common miRNAs targeting FLI1 3' UTR and circZNF609 with miRTarBase v8 identified high confidence miRNAs potentially involved in the circZNF609/EWS::FLI1/ miRNA regulatory axis.

3. Results

Characterizing CircZNF609 in EwS CircZNF609 (has_circ_0000615) is generated from exon 2 of the ZNF609 pre-mRNA and is 874 nucleotides in length (Figure 1A) (Legnini et al., 2017). We assessed circZNF609 expression in EwS using RT-qPCR and found it to be constitutively expressed at higher levels in the A673 and TC32 EwS cell lines compared to a control non-Ewing sarcoma cell line, specifically immortalized human myoblasts called AB678 (Figure 1B). The PCR product was validated by Sanger sequencing to confirm the presence of the back-splice junction (Figure 1C). Further validation using divergent primers and RNase R treatment (Suzuki et al., 2006; Vincent and Deutscher, 2006) showed that RNase R treatment of A673 RNA reduced linear ZNF609 levels, while circZNF609 expression persisted, confirming its circular nature; GAPDH was used as a control to demonstrate the effectiveness of RNase R on linear transcripts (Figure 1D). Conventional techniques

 doi:10.20944/preprints202511.2252.v1

for analyzing noncoding RNAs, including circRNAs, do not provide information about their cellular localization, which is important for understanding their function. We used our recently developed circFISH method (Koppula et al., 2022) to determine the cellular localization of circZNF609 in EwS cell lines (Figure 1E and H). The expression levels of circZNF609 were approximately half that of linear ZNF609 (Figure 1F), and both linear ZNF609 and circZNF609 were predominantly localized in the cytoplasm compared to the nucleus in both A673 and TC32 cells (Figure 1G). These findings suggest that circZNF609 may regulate EwS oncogenesis post-transcriptionally, potentially via miRNA or RNA-binding protein (RBP) sponging.

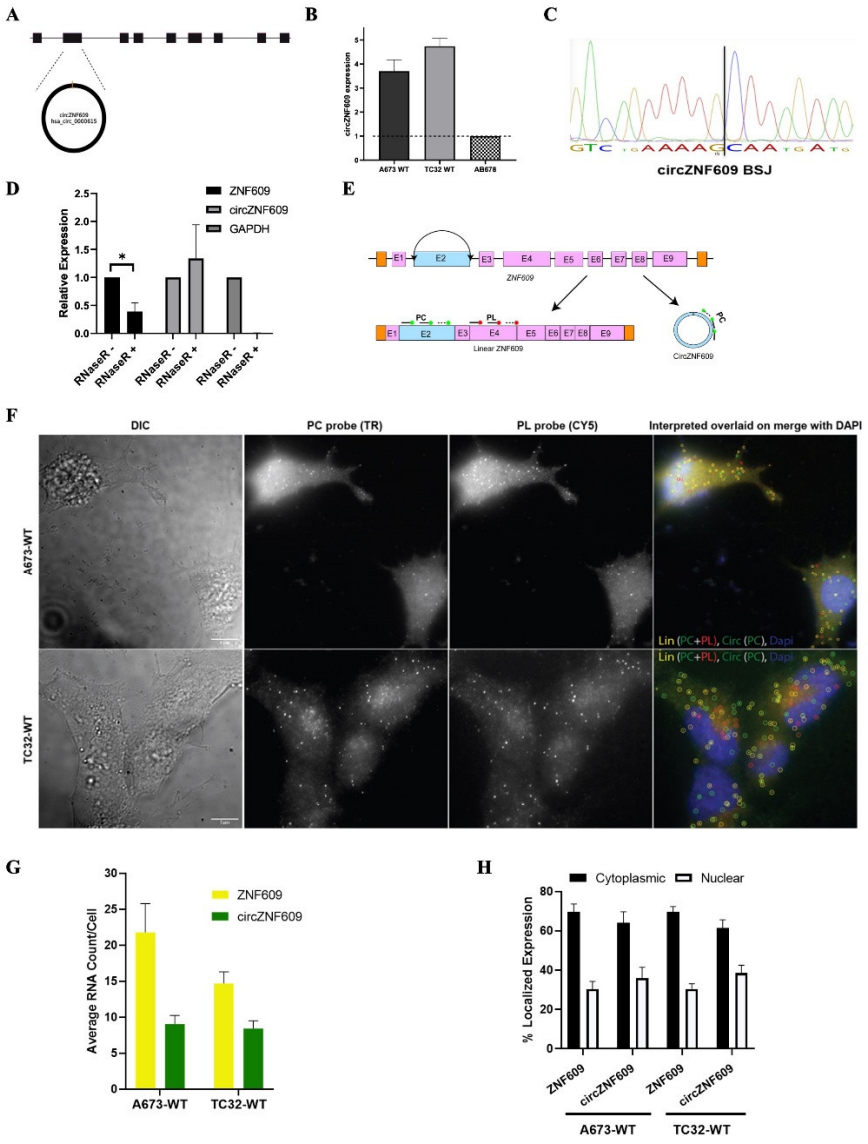

Figure 1. Validating the expression of circZNF609 in EwS cell lines: A. A representative image of the genomic location and backsplicing configuration of circZNF609 (has_circ_0000615). **B.** qRT-PCR data showing circZNF609 expression levels in EwS cell lines (A673 and TC32) and normal human muscle myoblast cell line (AB678). **C.** Sanger sequencing of the amplified PCR product of circZNF609 to confirm the unique BSJ. **D.** qRT-PCR analysis of A673 cells treated with RNase R demonstrating expression of linear ZNF609, circZNF609 and GAPDH (control) and normalized to mock RNase R treatment. The error bars indicate the standard deviation between triplicates. **E.** Schematic of circFISH assay. **F.** Representative image panel of circFISH for ZNF609 in A673 and TC32 cells with the PL and PC probes. From the left: DIC; raw merged z stacks of cells for PL probes labeled with TR; raw merged z stacks of cells for PC probes labeled with Cy5; and a merged image of the two channels with TR spots pseudo-colored red and Cy5 pseudo-colored green, overlaid on DAPI with MATLAB-interpreted spots. Full-length linear, circular and fragmented linear RNA is represented as yellow, green, and

 doi:10.20944/preprints202511.2252.v1

red spots, respectively. The scale bar is 5 μm. **G.** Quantification of ZNF609 and circZNF609 signals after MATLAB analysis. The columns represent the average ZNF609 and circZNF609 RNA molecules per cell, as analyzed in MATLAB across 2 cell lines. **H.** Average relative nuclear and cytoplasmic localization of ZNF609 and circZNF609 across 2 cell lines. The error bars indicate the 95% confidence interval for at least 100 cells. The error bars indicate the standard deviation between triplicates. * Indicates a significant difference with a p-value < 0.05.

3.1. Downregulation of CircZNF609 Impairs EwS Cell Proliferation, Tumorigenicity, and Viability

To understand the underlying molecular mechanism circZNF609 plays in regulating EwS, we performed a shRNA mediated knockdown of circZNF609 in A673 and TC32 cells by targeting the BSJ of circZNF609, and significant knockdown of circZNF609 in A673 and TC32 cells was measured by RT-qPCR (Figure 2).

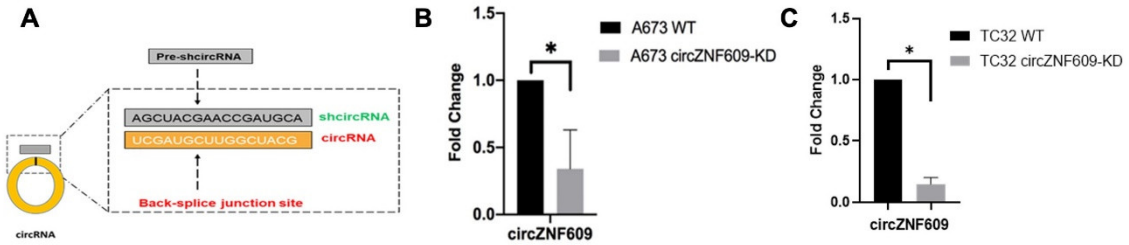

Figure 2. ShRNA mediated circZNF609 knockdown. A) Backsplice junction (BSJ) sequence specific shRNA designed to knockdown respective circRNA. **B&C)** qRT-PCR data showing circZNF609 fold change in wildtype and circZNF609 knockdown A673 and TC32 cells respectively. The error bars indicate the standard deviation between triplicates. * Indicates a significant difference with a p-value < 0.05.

To evaluate the effect of circZNF609 knockdown on the proliferative capacity of EwS cells, we performed MTT assays and observed a significant reduction in proliferation rate after 72 hours in TC32 cells and after 96 hours in A673 cells compared to wild-type (WT) cells (Figure 3A and B). Additionally, circZNF609 knockdown in both TC32 and A673 cells resulted in an increase in the number of apoptotic cells as seen in the late apoptotic (LA) and early apoptotic (EA) quadrants for Annexin V and PI double-positive cells,, indicating that circZNF609 knockdown induces apoptosis (Figure 3C and D). Furthermore, soft agar colony formation assays showed a significant reduction in the number of colonies formed by circZNF609-KD cells compared to WT cells (Figure 3E and F), indicating reduced tumorigenicity. In summary, circZNF609 knockdown impairs cell proliferation and tumor growth and induces apoptosis. These results are consistent with existing data reporting that circZNF609 functions as an oncogenic circRNA in other cancers (Qian et al., 2021; Rossi et al., 2019; Wang et al., 2021, 2022). Our results validated the oncogenic role on of circZNF609 in EwS for the first time.

 doi:10.20944/preprints202511.2252.v1

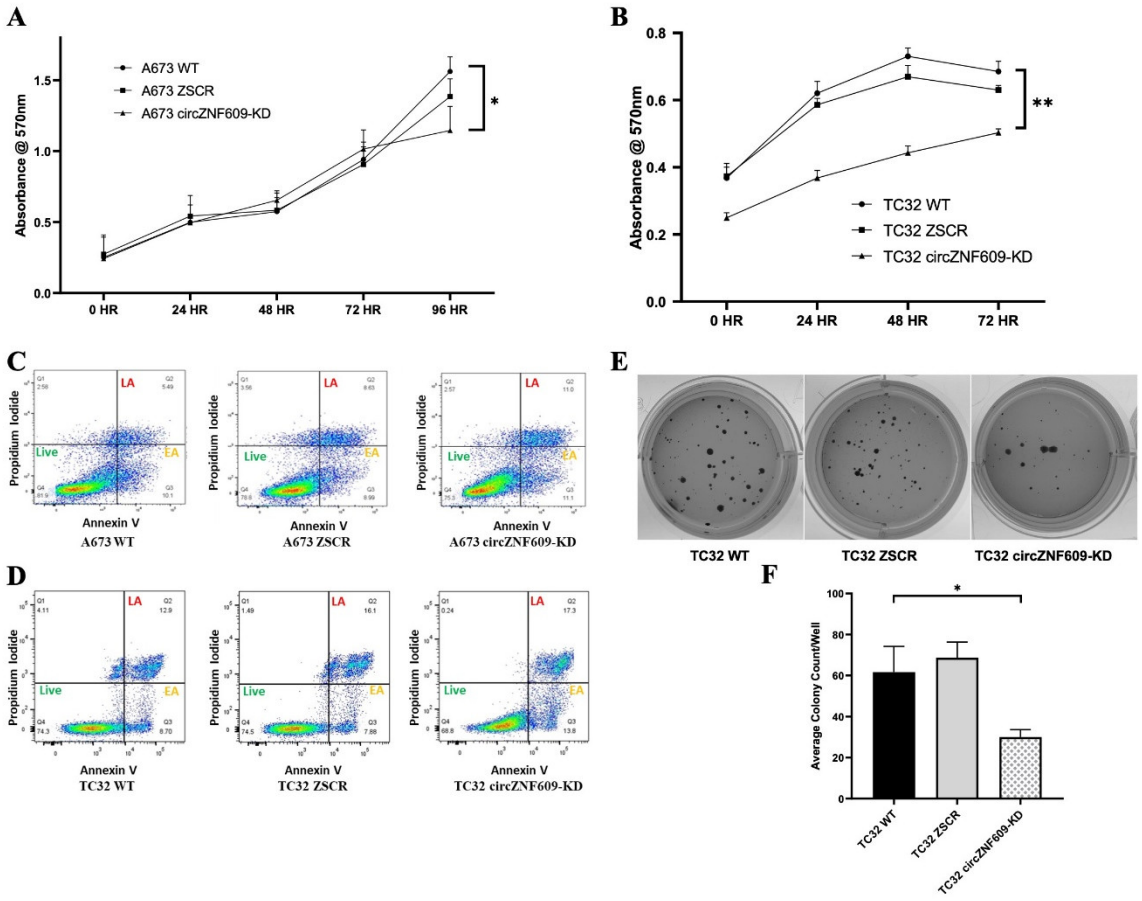

Figure 3. Functional effect of CircZNF609 knockdown in EwS: A and B. Line graph showing the average proliferation rate of A673WT, zSCR and circZNF609KD in A673 and TC32 cells using MTT assay for a period of 4 days with 24 hour reading intervals. **C and D**: Flow cytometry quadrant analysis distinguishing between healthy and apoptotic (Early apoptotic (EA) + Late apoptotic (LA) cells of A673 and TC32 (WT, ZSCR and circZNF609-KD) cell lines respectively based on their Annexin V and PI levels. Flow cytometry analysis was performed for 20,000 events (cells). **E**. Colonies on soft agar assay analyzed after 14-28 days. **F**. Bar graph showing the average colony count per 5000 cells in a 12well plate for TC32 WT, ZSCR and circZNF609-KD cells after 14 days. The error bars indicate the standard deviation between triplicates. * Indicates a significant difference with a p-value < 0.05.

3.2. Downregulation of CircZNF609 Reduced the Level of EWS::FLI1 Protein in EwS Cells

To investigate the mechanism by which circZNF609 exerts its functional effects, we examined whether it influences the levels of the oncogenic driver fusion protein EWS::FLI1. We first assessed EWS::FLI1 mRNA levels and found no significant difference between WT and circZNF609 knockdown cells, suggesting that circZNF609 does not affect EWS::FLI1 transcription (supplementary Figure 1). Given that circRNAs often regulate gene expression post-transcriptionally, we next evaluated EWS::FLI1 protein levels and observed a reduction in EWS::FLI1 protein in circZNF609 knockdown cell lines, as determined by both immunofluorescence (Figure 4A and B) and western blot analysis (Figure 4C and D). We also performed polysome fractionation and found a decreased association of EWS::FLI1 mRNA with polysomes in circZNF609 knockdown cells compared to WT cells (Figure 4E and F). An inducible EWS::FLI1 knockdown (EFKD) in A673 cells was used as a positive control. These findings further indicate that circZNF609 affects the translation of EWS::FLI1 mRNA.

 doi:10.20944/preprints202511.2252.v1

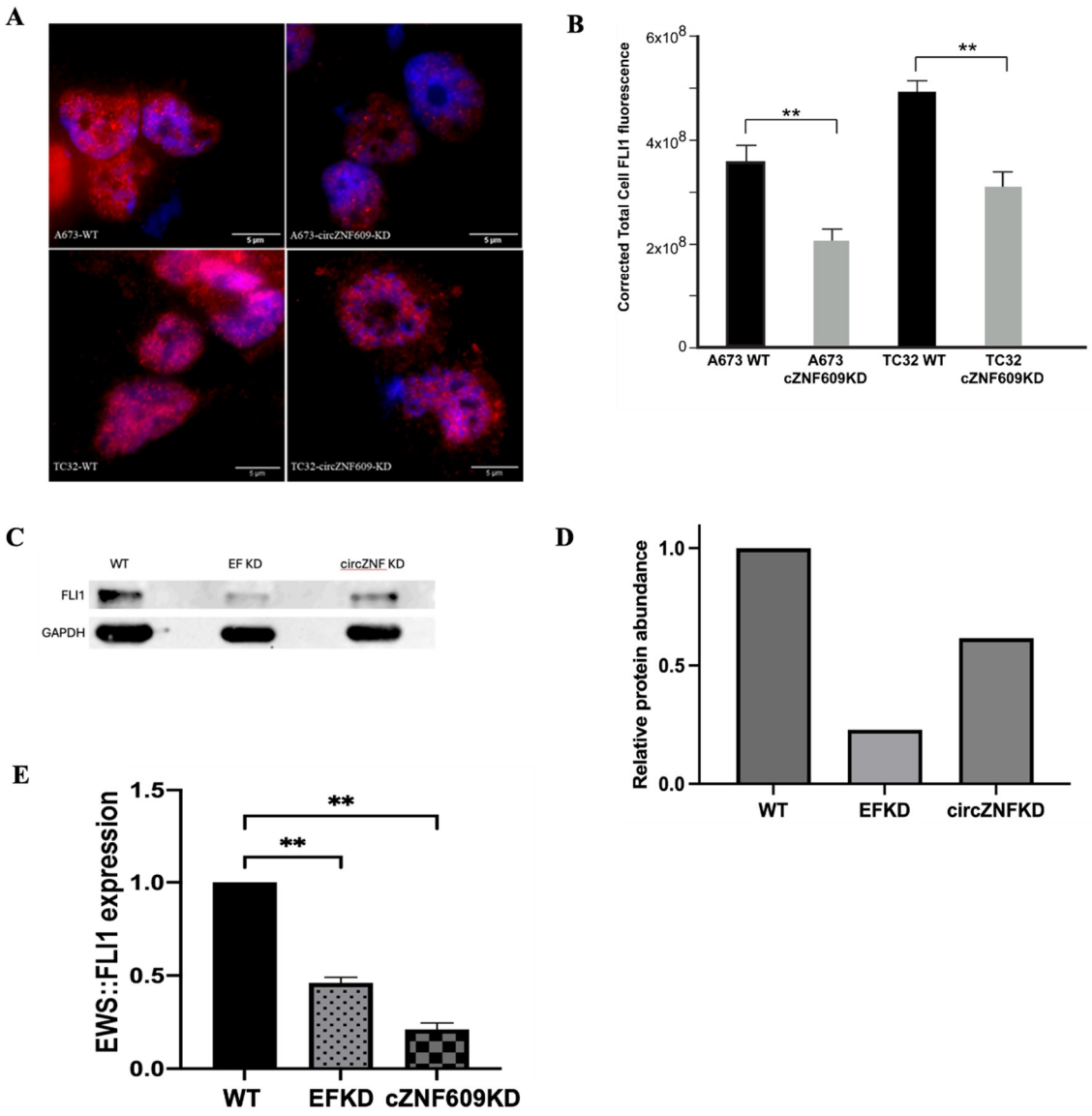

Figure 4. Downregulation of EWS::FLI1 protein levels in circZNF609 KD cells: A. Representative images of A673 and TC32 (WT and circZNF609-KD) cells. Raw merged z stacks of cells hybridized with FLI1 primary antibodies tagged with secondary AF647 antibodies (red) overlaid on DAPI (blue). The scale bar is 5 μm. **B.** Corrected total cell fluorescence (CTCF) of FLI1 protein (representing EWS::FLI1) in TC32 cells (WT, ZSCR [negative control] and circZNF609-KD) respectively. The error bars indicate the 95% confidence interval for at least 70 cells. **C**. Western blot analysis for EWS::FLI1 protein expression across A673 (WT, EFKD, circZNF609-KD, and ZSCR) cells using anti-FLI1 antibody, GAPDH as loading control. **D.** Bar graph showing EWS::FLI1 protein expression levels from western blot across A673 cells (WT, EFKD, circZNF609-KD, and ZSCR). **E.** qRT-PCR data showing the EWS::FLI1 expression in the polysome fraction obtained using size exclusion chromatography (SEC). of A673 cells (WT, EF-KD and circZNF609-KD). Error bars indicate the standard deviation between triplicates. ** Indicates a significant difference with a p-value < 0.005.

Mechanism of EWS::FLI1 down regulation by circZNF609: Since the most well-studied function of circRNAs is mediated by sponging of miRNAs (Hansen et al., 2013; Memczak et al., 2013; Panda, 2018), we investigated whether a similar regulatory mechanism occurs in EwS cells. Several miRNAs have been reported in the literature to be differentially regulated by EWS::FLI1, although not all directly inhibit EWS::FLI1 expression (Mosakhani et al., 2012). Likewise, many miRNAs have been reported to be sponged by circZNF609 in various cancers (Du et al., 2021; Ghadami et al., 2024; Qian et al., 2021; Ren et al., 2024; Wang et al., 2022, 2018). Given the observed reduction of EWS::FLI1 protein in circZNF609 knockdown cells, we aimed to identify miRNAs that both bind to EWS::FLI1

 doi:10.20944/preprints202511.2252.v1

and have binding sites on circZNF609. Using TargetScan and miRDB, we identified 152 miRNAs predicted to bind the 3′ UTR of EWS::FLI1 and found in both the databases (Figure 5A), which we further narrowed down to 46 which are functionally relevant miRNAs using miRDB (Figure 5B). We then identified all the miRNAs predicted to have a binding site for circZNF609 and compared them to all miRNAs predicted to bind FLI1 3′UTR. Finally, we compared this analysis to the miRTarBase v8 hg to find which of these common miRNAs are reported to be expressed in Human cells and identified 7 common miRNAs (Figure 5C). All 7 were tested by qRT-PCR to determine their levels in EwS cells, and we found that miR-145-5p showed the most significant EWS::FLI1-dependent expression (Figure 5C). Numerous studies have reported that circZNF609 acts by sponging miR-145-5p, as seen in glioblastoma (Ghadami et al., 2024; Liu et al., 2019; Wang et al., 2018). Furthermore, miR-145-5p is a key miRNA in EwS, and its reduction has been reported to promote oncogenesis in EwS via a yet unknown mechanism (Ban et al., 2011; Guzel Tanoglu and Ozturk, 2021). Finally, miR145-5p has been shown to regulate the expression of FLI1 in osteosarcoma (Chen et al., 2021).

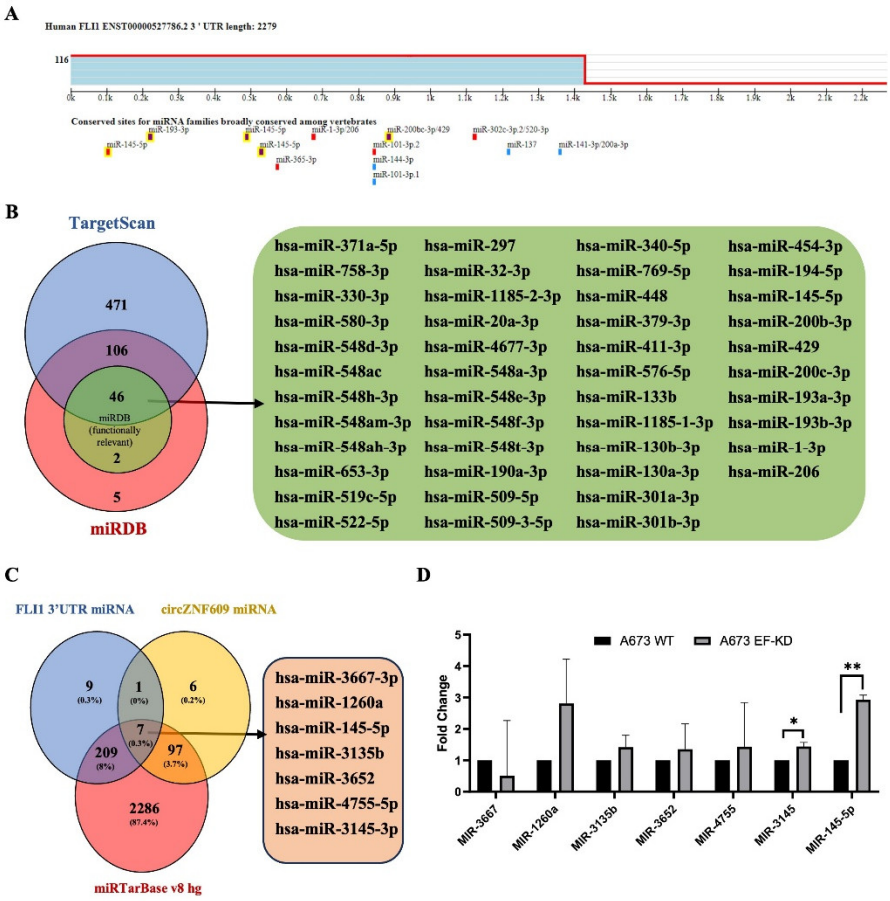

Figure 5. miRNAs targeting EWS::FLI1 and sponged by circZNF609. A. Conserved miRNA binding sites prediction for FLI1 3′ UTR using TargetScan. **B.** Common miRNAs predicted to bind FLI1 3′UTR from TargetScan and miRDB. Functionally relevant miRNAs denoted in green. List of all the functionally relevant miRNAs predicted to target FLI1 3′UTR from TargetScan and miRDB. C. Common miRNAs predicted to bind FLI1 3′UTR, circZNF609 and reported in miRTarBase. **D.** qRT-PCR data showing fold change of miRNAs in A673 WT and A673 EF-KD cells with common binding elements in FLI1 3′UTR and circZNF609). The error bars indicate the standard deviation between triplicates. * Indicates a significant difference with a p-value < 0.05. ** Indicates a significant difference with a p-value < 0.005.

Direct visualization of circZNF609 and miR145-5p interaction: To directly visualize the interaction between circZNF609 and miR-145-5p, we combined our circFISH assay with miRNA imaging to assess their co-localization. CircZNF609 was detected using probes labeled with Cy5, and after hybridization with circFISH probes, cells were further stained with miRNA probes requiring

 doi:10.20944/preprints202511.2252.v1

signal amplification. We observed that a subset of circZNF609 RNA molecules co-localized with the miR-145-5p signal. Although the signals were somewhat diminished due to multiple rounds of washing, staining, and signal processing, the data clearly demonstrate that circZNF609 has a binding site for miR-145-5p and that this interaction occurs in A673 cells (Figure 6).

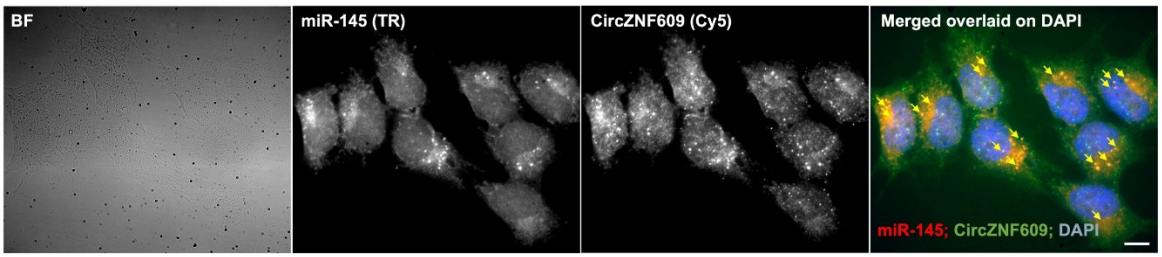

Figure 6. Simultaneous staining of circRNA and miRNA: Representative image panel of A673 cells hybridized with antibodies for miR-145 (TR) and probes for ZNF609 (Cy5). A merged image of the two channels with miR-145 spots pseudo-colored in red and ZNF609 pseudo-colored in green, overlaid on DAPI. Yellow arrows point to the colocalization between miR-145 and circZNF609. The scale bar is 5um.

Functional validation of role of circZNF609 sponging miR145-5p in EwS: It is well established that miR-145-5p is significantly repressed by EWS::FLI1 and functions in a feedback regulatory loop in EwS, although the mechanism of miR-145-5p suppression is not understood (Ban et al., 2011; Cui et al., 2014; Fan et al., 2012). Interestingly, we observed a reduction in circZNF609 levels in EWS::FLI1 knockdown (EFKD) cells, indicating that its expression is positively correlated with EWS::FLI1 (Figure 7A). Consistent with existing literature, miR-145-5p levels showed a significant increase in EFKD cells (Figure 7B), but there was no reduction in miR-145-5p levels in circZNF609 knockdown cells, suggesting that circZNF609 does not regulate the expression of miR-145-5p (Figure 7C) (Ban et al., 2011). This is not unexpected, as circRNAs typically do not affect the expression but rather the function of their target miRNAs (Silenzi et al., 2024). To assess the impact of circZNF609 on miR-145-5p function, we performed a luciferase assay by cloning two fragments of the FLI1 3′ UTR into the psiCHECK2 vector downstream of the Renilla luciferase coding region. Fragment 1 contains the binding site for miR-145-5p, while fragment 2 does not (Figure 7D). TC32 cells (WT, ZSCR, and circZNF609-KD) were transfected with these constructs, along with empty and mock controls. We observed a change in luciferase expression only with FLI1 3′ UTR fragment 1, with reduced luciferase activity in circZNF609-KD cellswhile fragment 2 remained unchanged (Figure 7E), suggesting that circZNF609 sponges miR-145-5p. Addition of a miR-145-5p mimic showed a dose-dependent response in TC32 WT cells (Figure 7F), while addition of a negative control mimic did not affect luciferase activity (Figure 7G), further confirming that the effect is specific to miR-145 binding to the 3′ UTR, which is also a target of circZNF609. Together, the direct visualization of the circRNA:miRNA interaction and the functional luciferase assay confirm the circZNF609–miR-145–EWS::FLI1 regulatory axis in EwS.

 doi:10.20944/preprints202511.2252.v1

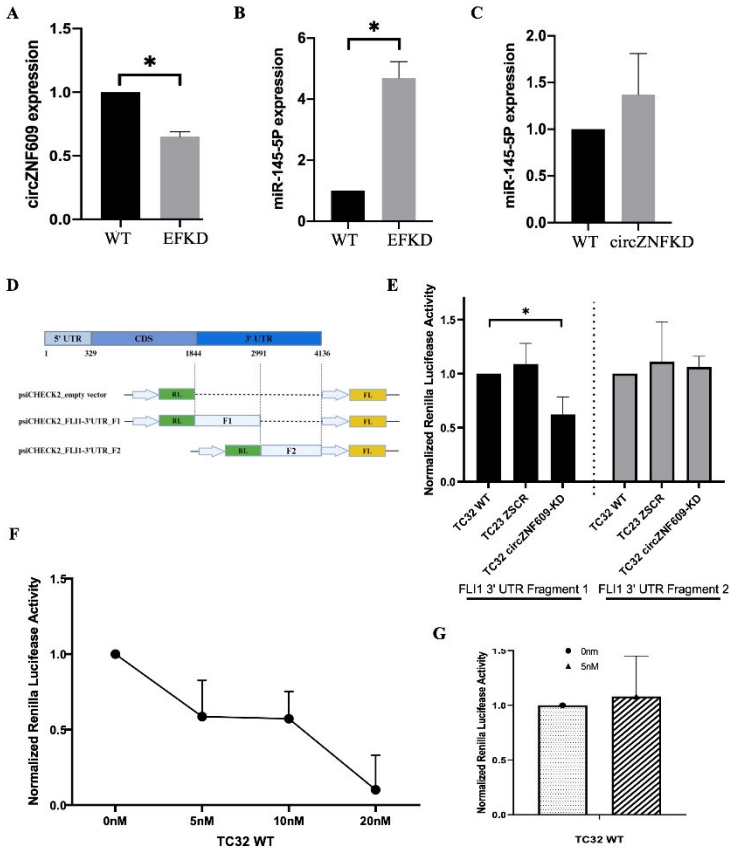

Figure 7. Function validation of circZNF609 regulating miR145 function in EwS: A. qRT-PCR to quantify the expression of circZNF609 in A673 WT and EFKD cells. **B.** Expression of miR145-5p in A673WT and EFKD. **C.** Expression of miR145-5p in A673WT and CIRCZNFKD cells. **D**. Schematic of luciferase construct expressing fragments of FLI1 3'UTR. **E.** Dose response curve of luciferase activity upon addition of a miR145 mimic in TC32 WT cells. **F.** Luciferase activity upon addition of a negative control miRNA mimic in TC32 WT cells. The error bars indicate the standard deviation between triplicates. * Indicates a significant difference with a p-value < 0.05.

circZNF609 function as a regulatory RNA in EwS: Although circRNAs are generally classified as non-coding RNAs, a few have been shown to be translated into short peptides via cap-independent mechanisms such as internal ribosome entry sites (Hwang and Kim, 2024). Notably, circZNF609 is among the few circRNAs with demonstrated coding potential, and its peptide has been shown to have functional roles in myogenesis and acute kidney disease (Legnini et al., 2017; Ouyang et al., 2023). This prompted us to investigate whether the peptide form of circZNF609 plays a role in EwS. We performed polysome fractionation and found no significant changes in the association of circZNF609 RNA with polysome fractions among WT, EFKD, and circZNF609KD cells, suggesting that if the peptide is produced, it does not play a functional role in EwS. These results confirm that circZNF609 functions as a regulatory RNA in EwS (supplementary Figure 2).

4. Discussion

Over the past decade, ample evidence has demonstrated the impact of circRNAs on the development and progression of various diseases, particularly human cancers such as lung, prostate, colon, breast, and hepatocellular carcinomas, as well as osteosarcoma (D'Ambra et al., 2019; Guo et al., 2022; Qian et al., 2021; Soghli et al., 2020; Su et al., 2019; Wang et al., 2022; Yang et al., 2020; Zhang et al., 2020). CircRNAs are highly stable due to their resistance to exonucleases and have been detected in extracellular vesicles and bodily fluids, making them promising candidates for biomarkers and therapeutics (Abdelgawad et al., 2025; Hoque et al., 2023; Li et al., 2018; Su et al., 2019).

 doi:10.20944/preprints202511.2252.v1

CircZNF609 is a very well-studied oncogenic circRNA (Wang et al., 2022). Existing research has demonstrated the importance of circZNF609 in regulating cell proliferation, migration, and metastasis in several human malignancies, including hepatocellular carcinoma, breast cancer, lung adenocarcinoma, gastric cancer, and glioma (He et al., 2020; Liu et al., 2021; Wang et al., 2022, 2018; Wu et al., 2018). However, the expression and function of circZNF609 have not previously been reported in EwS. Here, we present the first characterization of a functional circular RNA in EwS. We validated the expression, role, and mechanism of action of circZNF609 in EwS and identified the circZNF609:miR-145-5p:FLI1 regulatory axis. Our data show that circZNF609 is expressed in an EWS::FLI1-dependent manner, and it is well established that miR-145-5p is a critical miRNA capable of suppressing EWS::FLI1 expression. Furthermore, FLI1 is not expressed in normal cells, which is why EWS::FLI1 is often detected and studied using antibodies against the 3′ end of FLI1 (Melot et al., 1997). Integrating our new functional data with existing studies, we propose a model in which, under normal conditions, cells express miR-145-5p, which binds to the 3′ UTR of FLI1 and keeps EWS::FLI1 translationally inhibited after the translocation occurs. However, as EWS::FLI1 expression increases, its concentration likely surpasses the regulatory capacity of miR-145-5p, allowing EWS::FLI1 protein to accumulate. Early expression of EWS::FLI1 induces circZNF609 and other effectors that repress miR-145-5p expression by yet unknown mechanisms. The expression of circZNF609 leads to sponging of miR-145-5p, thereby blocking its function and enabling higher levels of EWS::FLI1 protein, which in turn promotes aberrant gene expression and increases proliferation, invasiveness, and growth in EwS (Figure8). This positive feedback loop ensures that EWS::FLI1 protein concentrations remain high in the cells, representing a novel strategy by which EWS::FLI1 evades repression by miRNAs.

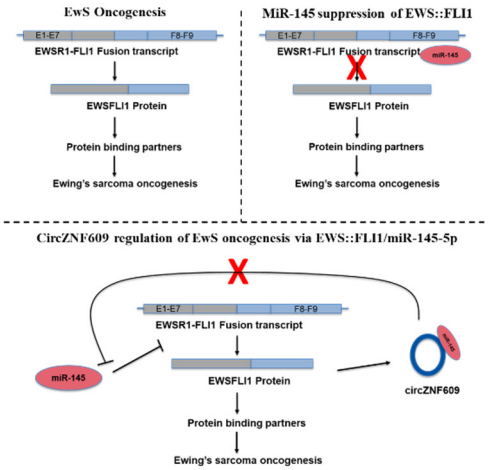

Figure 8. EWS::FLI1 recruits circZNF69 to repress miR145-5p function: Proposed model for EWS::FLI1 regulation by circZNF609 in EwS showing under normal conditions, miR145-5p degrades the EWS::FLI1 mRNA that upon expression of EWS::FLI1 protein, circZNf609 is upregulated, which sponges the miR145-5p and de repressing its effect and thus high amounts of EWS::FLI1 is achieved in the cell promoting oncogenesis in EwS.

This is the first report describing the role of circular RNAs in EwS. A recent work by Chen et al. has reported another circRNA called circCAMSAP1 to sponge miR-145 to de-repress FLI1 expression in Osteosarcoma in both cell lines and animal models providing a comparative perspective on circRNA functions across different sarcomas as well as the biological relevance of reducing miR145-FLI1 interaction (Chen et al., 2021); however, this circRNA has not been identified in EwS cell lines. Through genome profiling, we identified more circRNAs, of which several including circZNF609, are upregulated and some are downregulated in EwS, indicating diverse functional roles for these regulatory RNAs that remain to be explored (unpublished data). We acknowledge that a limitation of this study is the lack of analysis of circZNF609 levels in patient samples. Future studies are planned to test the expression of circZNF609 in patient samples as well to functionally characterize the role of

 doi:10.20944/preprints202511.2252.v1

other circRNAs. A recent study showed that EWS::FLI1 is not just a "rogue" transcription factor (regulating gene expression at the DNA level), but it also functions independently as an mRNA decay factor (regulating the lifespan of genetic messages) (Galvan et al., 2025). By identifying and characterizing the mechanism of action of the first circular RNA in EwS, our study provides another possible function of EWS::FLI1 as a "miRNA silencer" and will set the foundation for future research aimed at developing better diagnostic markers and therapeutic targets for EwS.

Author Contributions: AK: Investigation, data curation, analysis, methodology, article writing, review, and editing AA: Investigation, data curation, analysis, methodology, article writing, review, and editing. VB: Methodology, review, and editing. VP: Funding acquisition, review, editing. MB: Conceptualization, supervision, analysis, funding acquisition, project administration, article writing, review, and editing.

Funding: This research was funded by National Science Foundation, grant number 2244127 to M.B. and V.P.

Institutional Review Board Statement: N/A.

Informed Consent Statement: N/A.

Data Availability Statement: N/A.

Acknowledgments: We would like to thank the members of Batish Laboratory for their discussion and support. We are also thankful to Dr. Amaresh Panda and his group for help in the bioinformatic analysis of miRNA: circRNA binding sites.

Permission to Reproduce Material from Other Sources: N/A.

Clinical trial registration: N/A.

Conflicts of Interest: N/A.

References

Abdelgawad, A., Huang, Y., Gololobova, O., Yu, Y., Witwer, K.W., Parashar, V., Batish, M., 2025. Defining the Parameters for Sorting of RNA Cargo Into Extracellular Vesicles. Journal of Extracellular Vesicles 14, e70113. https://doi.org/10.1002/jev2.70113

Ban, J., Jug, G., Mestdagh, P., Schwentner, R., Kauer, M., Aryee, D.N.T., Schaefer, K.-L., Nakatani, F., Scotlandi, K., Reiter, M., Strunk, D., Speleman, F., Vandesompele, J., Kovar, H., 2011. Hsa-mir-145 is the top EWS-FLI1-repressed microRNA involved in a positive feedback loop in Ewing's sarcoma. Oncogene 30, 2173–2180. https://doi.org/10.1038/onc.2010.581

Barrett, C., Budhiraja, A., Parashar, V., Batish, M., 2021. The Landscape of Regulatory Noncoding RNAs in Ewing's Sarcoma. Biomedicines 9, 933. https://doi.org/10.3390/biomedicines9080933

Batish, M., Tyagi, S., 2019. Fluorescence In Situ Imaging of Dendritic RNAs at Single-Molecule Resolution. Curr Protoc Neurosci 89, e79. https://doi.org/10.1002/cpns.79

Chen, Y., Wang, X., 2020. miRDB: an online database for prediction of functional microRNA targets. Nucleic Acids Res 48, D127–D131. https://doi.org/10.1093/nar/gkz757

Chen, Z., Xu, W., Zhang, D., Chu, J., Shen, S., Ma, Y., Wang, Q., Liu, G., Yao, T., Huang, Y., Ye, H., Wang, J., Ma, J., Fan, S., 2021. circCAMSAP1 promotes osteosarcoma progression and metastasis by sponging miR-145-5p and regulating FLI1 expression. Mol Ther Nucleic Acids 23, 1120–1135. https://doi.org/10.1016/j.omtn.2020.12.013

Cui, S.-Y., Wang, R., Chen, L.-B., 2014. MicroRNA-145: a potent tumour suppressor that regulates multiple cellular pathways. J Cell Mol Med 18, 1913–1926. https://doi.org/10.1111/jcmm.12358

D'Ambra, E., Capauto, D., Morlando, M., 2019. Exploring the Regulatory Role of Circular RNAs in Neurodegenerative Disorders. Int J Mol Sci 20, 5477. https://doi.org/10.3390/ijms20215477

Deng, Q., Natesan, R., Cidre-Aranaz, F., Arif, S., Liu, Y., Rasool, R.U., Wang, P., Mitchell-Velasquez, E., Das, C.K., Vinca, E., Cramer, Z., Grohar, P.J., Chou, M., Kumar-Sinha, C., Weber, K., Eisinger-Mathason, T.S.K., Grillet,

 doi:10.20944/preprints202511.2252.v1

N., Grünewald, T.G.P., Asangani, I.A., 2022. Oncofusion-driven de novo enhancer assembly promotes malignancy in Ewing sarcoma via aberrant expression of the stereociliary protein LOXHD1. Cell Rep 39, 110971. https://doi.org/10.1016/j.celrep.2022.110971

Derrien, T., Johnson, R., Bussotti, G., Tanzer, A., Djebali, S., Tilgner, H., Guernec, G., Martin, D., Merkel, A., Knowles, D.G., Lagarde, J., Veeravalli, L., Ruan, X., Ruan, Y., Lassmann, T., Carninci, P., Brown, J.B., Lipovich, L., Gonzalez, J.M., Thomas, M., Davis, C.A., Shiekhattar, R., Gingeras, T.R., Hubbard, T.J., Notredame, C., Harrow, J., Guigó, R., 2012. The GENCODE v7 catalog of human long noncoding RNAs: analysis of their gene structure, evolution, and expression. Genome Res 22, 1775–1789. https://doi.org/10.1101/gr.132159.111

Du, F., Zhao, X., Fan, D., 2017. Soft Agar Colony Formation Assay as a Hallmark of Carcinogenesis. Bio Protoc 7, e2351. https://doi.org/10.21769/BioProtoc.2351

Du, S., Li, H., Lu, F., Zhang, S., Tang, J., 2021. Circular RNA ZNF609 promotes the malignant progression of glioma by regulating miR-1224-3p/PLK1 signaling. J Cancer 12, 3354–3366. https://doi.org/10.7150/jca.54934

Dudekula, D.B., Panda, A.C., Grammatikakis, I., De, S., Abdelmohsen, K., Gorospe, M., 2016. CircInteractome: A web tool for exploring circular RNAs and their interacting proteins and microRNAs. RNA Biol 13, 34–42. https://doi.org/10.1080/15476286.2015.1128065

Fan, L., Wu, Q., Xing, X., Wei, Y., Shao, Z., 2012. MicroRNA-145 targets vascular endothelial growth factor and inhibits invasion and metastasis of osteosarcoma cells. Acta Biochim Biophys Sin (Shanghai) 44, 407–414. https://doi.org/10.1093/abbs/gms019

Fan, Z., Dong, S., Wang, N., Khawar, M.B., Wang, J., Sun, H., 2024. Unlocking epigenetics for precision treatment of Ewing's sarcoma. Chin J Cancer Res 36, 322–340. https://doi.org/10.21147/j.issn.1000-9604.2024.03.08

Figuerola-Bou, E., Ríos-Astorch, C., Blanco, E., Sánchez-Jiménez, M., Táboas, P., Fernández, G., Gómez-González, S., Muñoz, O., Castellano-Escuder, P., Perez-Jaume, S., Garcia, M., Prada, E., Mateo-Lozano, S., Riggi, N., Avgustinova, A., Lavarino, C., Di Croce, L., Sánchez-Molina, S., Mora, J., 2025. KDM6 Demethylases Contribute to EWSR1::FLI1-Driven Oncogenic Reprogramming in Ewing Sarcoma. Cancer Res 85, 4485–4503. https://doi.org/10.1158/0008-5472.CAN-24-3452

Galvan, B., Ongena, L., Bruyr, J., Fettweis, G., Lucarelli, E., Lavergne, A., Mariavelle, E., O'Grady, T.M., Hassoun, Z.E.O., Claes, M., Dubois, L., Lee, K.A.W., Kruys, V., Gueydan, C., Durand, J., Hervouet, E., Geyer, F.H., Banito, A., Imle, R., Mao, L., Jayavelu, A.K., Grünewald, T.G.P., Cidre-Aranaz, F., Twizere, J.-C., Dequiedt, F., 2025. Subversion of mRNA degradation pathways by EWSR1::FLI1 represents a therapeutic vulnerability in Ewing sarcoma. Nat Commun 16, 6537. https://doi.org/10.1038/s41467-025-61725-x

Ghadami, E., Gorji, A., Pour-Rashidi, A., Noorbakhsh, F., Kabuli, M., Razipour, M., Choobineh, H., Maghsudlu, M., Damavandi, E., Ghadami, M., 2024. CircZNF609 and circNFIX as possible regulators of glioblastoma pathogenesis via miR-145-5p/EGFR axis. Sci Rep 14, 13551. https://doi.org/10.1038/s41598-024-63827-w

Grünewald, T.G.P., Cidre-Aranaz, F., Surdez, D., Tomazou, E.M., de Álava, E., Kovar, H., Sorensen, P.H., Delattre, O., Dirksen, U., 2018. Ewing sarcoma. Nat Rev Dis Primers 4, 5. https://doi.org/10.1038/s41572-018-0003-x

Guo, L., Jia, L., Luo, L., Xu, X., Xiang, Y., Ren, Y., Ren, D., Shen, L., Liang, T., 2022. Critical Roles of Circular RNA in Tumor Metastasis via Acting as a Sponge of miRNA/isomiR. Int J Mol Sci 23, 7024. https://doi.org/10.3390/ijms23137024

Guzel Tanoglu, E., Ozturk, S., 2021. miR-145 suppresses epithelial-mesenchymal transition by targeting stem cells in Ewing sarcoma cells. Bratisl Lek Listy 122, 71–77. https://doi.org/10.4149/BLL_2021_009

Hansen, T.B., Jensen, T.I., Clausen, B.H., Bramsen, J.B., Finsen, B., Damgaard, C.K., Kjems, J., 2013. Natural RNA circles function as efficient microRNA sponges. Nature 495, 384–388. https://doi.org/10.1038/nature11993

He, Y., Huang, H., Jin, L., Zhang, F., Zeng, M., Wei, L., Tang, S., Chen, D., Wang, W., 2020. CircZNF609 enhances hepatocellular carcinoma cell proliferation, metastasis, and stemness by activating the Hedgehog pathway through the regulation of miR-15a-5p/15b-5p and GLI2 expressions. Cell Death Dis 11, 358. https://doi.org/10.1038/s41419-020-2441-0

Hoque, P., Romero, B., Akins, R.E., Batish, M., 2023. Exploring the Multifaceted Biologically Relevant Roles of circRNAs: From Regulation, Translation to Biomarkers. Cells 12, 2813. https://doi.org/10.3390/cells12242813

 doi:10.20944/preprints202511.2252.v1

Hwang, H.J., Kim, Y.K., 2024. Molecular mechanisms of circular RNA translation. Exp Mol Med 56, 1272–1280. https://doi.org/10.1038/s12276-024-01220-3

Jeck, W.R., Sorrentino, J.A., Wang, K., Slevin, M.K., Burd, C.E., Liu, J., Marzluff, W.F., Sharpless, N.E., 2013. Circular RNAs are abundant, conserved, and associated with ALU repeats. RNA 19, 141–157. https://doi.org/10.1261/rna.035667.112

Koppula, A., Abdelgawad, A., Guarnerio, J., Batish, M., Parashar, V., 2022. CircFISH: A Novel Method for the Simultaneous Imaging of Linear and Circular RNAs. Cancers (Basel) 14, 428. https://doi.org/10.3390/cancers14020428

Kristensen, L.S., Andersen, M.S., Stagsted, L.V.W., Ebbesen, K.K., Hansen, T.B., Kjems, J., 2019. The biogenesis, biology and characterization of circular RNAs. Nat Rev Genet 20, 675–691. https://doi.org/10.1038/s41576-019-0158-7

Legnini, I., Di Timoteo, G., Rossi, F., Morlando, M., Briganti, F., Sthandier, O., Fatica, A., Santini, T., Andronache, A., Wade, M., Laneve, P., Rajewsky, N., Bozzoni, I., 2017. Circ-ZNF609 Is a Circular RNA that Can Be Translated and Functions in Myogenesis. Mol Cell 66, 22-37.e9. https://doi.org/10.1016/j.molcel.2017.02.017

Li, Y., Zeng, X., He, J., Gui, Y., Zhao, S., Chen, H., Sun, Q., Jia, N., Yuan, H., 2018. Circular RNA as a biomarker for cancer: A systematic meta-analysis. Oncol Lett 16, 4078–4084. https://doi.org/10.3892/ol.2018.9125

Liu, S., Yang, N., Jiang, X., Wang, J., Dong, J., Gao, Y., 2021. FUS-induced circular RNA ZNF609 promotes tumorigenesis and progression via sponging miR-142-3p in lung cancer. J Cell Physiol 236, 79–92. https://doi.org/10.1002/jcp.29481

Liu, Z., Pan, H.-M., Xin, L., Zhang, Y., Zhang, W.-M., Cao, P., Xu, H.-W., 2019. Circ-ZNF609 promotes carcinogenesis of gastric cancer cells by inhibiting miRNA-145-5p expression. Eur Rev Med Pharmacol Sci 23, 9411–9417. https://doi.org/10.26355/eurrev_201911_19433

May, W.A., Gishizky, M.L., Lessnick, S.L., Lunsford, L.B., Lewis, B.C., Delattre, O., Zucman, J., Thomas, G., Denny, C.T., 1993a. Ewing sarcoma 11;22 translocation produces a chimeric transcription factor that requires the DNA-binding domain encoded by FLI1 for transformation. Proc Natl Acad Sci U S A 90, 5752–5756. https://doi.org/10.1073/pnas.90.12.5752

May, W.A., Lessnick, S.L., Braun, B.S., Klemsz, M., Lewis, B.C., Lunsford, L.B., Hromas, R., Denny, C.T., 1993b. The Ewing's sarcoma EWS/FLI-1 fusion gene encodes a more potent transcriptional activator and is a more powerful transforming gene than FLI-1. Mol Cell Biol 13, 7393–7398. https://doi.org/10.1128/mcb.13.12.7393-7398.1993

McCloy, R.A., Rogers, S., Caldon, C.E., Lorca, T., Castro, A., Burgess, A., 2014. Partial inhibition of Cdk1 in G 2 phase overrides the SAC and decouples mitotic events. Cell Cycle 13, 1400–1412. https://doi.org/10.4161/cc.28401

McGeary, S.E., Lin, K.S., Shi, C.Y., Pham, T.M., Bisaria, N., Kelley, G.M., Bartel, D.P., 2019. The biochemical basis of microRNA targeting efficacy. Science 366, eaav1741. https://doi.org/10.1126/science.aav1741

McKinsey, E.L., Parrish, J.K., Irwin, A.E., Niemeyer, B.F., Kern, H.B., Birks, D.K., Jedlicka, P., 2011. A novel oncogenic mechanism in Ewing sarcoma involving IGF pathway targeting by EWS/Fli1-regulated microRNAs. Oncogene 30, 4910–4920. https://doi.org/10.1038/onc.2011.197

Melot, T., Gruel, N., Doubeikovski, A., Sevenet, N., Teillaud, J.L., Delattre, O., 1997. Production and characterization of mouse monoclonal antibodies to wild-type and oncogenic FLI-1 proteins. Hybridoma 16, 457–464. https://doi.org/10.1089/hyb.1997.16.457

Memczak, S., Jens, M., Elefsinioti, A., Torti, F., Krueger, J., Rybak, A., Maier, L., Mackowiak, S.D., Gregersen, L.H., Munschauer, M., Loewer, A., Ziebold, U., Landthaler, M., Kocks, C., le Noble, F., Rajewsky, N., 2013. Circular RNAs are a large class of animal RNAs with regulatory potency. Nature 495, 333–338. https://doi.org/10.1038/nature11928

Mosakhani, N., Guled, M., Leen, G., Calabuig-Fariñas, S., Niini, T., Machado, I., Savola, S., Scotlandi, K., López-Guerrero, J.A., Llombart-Bosch, A., Knuutila, S., 2012. An integrated analysis of miRNA and gene copy numbers in xenografts of Ewing's sarcoma. J Exp Clin Cancer Res 31, 24. https://doi.org/10.1186/1756-9966-31-24

Ouyang, X., He, Z., Fang, H., Zhang, H., Yin, Q., Hu, L., Gao, F., Yin, H., Hao, T., Hou, Y., Wu, Q., Deng, J., Xu, J., Wang, Y., Chen, C., 2023. A protein encoded by circular ZNF609 RNA induces acute kidney injury by

activating the AKT/mTOR-autophagy pathway. Mol Ther 31, 1722–1738. https://doi.org/10.1016/j.ymthe.2022.09.007

Panda, A.C., 2018. Circular RNAs Act as miRNA Sponges. Adv Exp Med Biol 1087, 67–79. https://doi.org/10.1007/978-981-13-1426-1_6

Qian, Y., Li, Y., Li, R., Yang, T., Jia, R., Ge, Y.-Z., 2021. circ-ZNF609: A potent circRNA in human cancers. J Cell Mol Med 25, 10349–10361. https://doi.org/10.1111/jcmm.16996

Ren, L., Huo, X., Zhao, Y., 2024. CircZNF609/miR-324-5p/voltage-dependent anion channel 1 axis promotes malignant progression of ovarian cancer cells. iScience 27, 110861. https://doi.org/10.1016/j.isci.2024.110861

Rossi, F., Legnini, I., Megiorni, F., Colantoni, A., Santini, T., Morlando, M., Di Timoteo, G., Dattilo, D., Dominici, C., Bozzoni, I., 2019. Circ-ZNF609 regulates G1-S progression in rhabdomyosarcoma. Oncogene 38, 3843–3854. https://doi.org/10.1038/s41388-019-0699-4

Silenzi, V., D'Ambra, E., Santini, T., D'Uva, S., Setti, A., Salvi, N., Nicoletti, C., Scarfò, R., Cordella, F., Mongiardi, B., Cavezza, D., Liessi, N., Ferrucci, L., Ragozzino, D., Armirotti, A., Di Angelantonio, S., De Leonibus, E., Bozzoni, I., Morlando, M., 2024. A tripartite circRNA/mRNA/miRNA interaction regulates glutamatergic signaling in the mouse brain. Cell Rep 43, 114766. https://doi.org/10.1016/j.celrep.2024.114766

Soghli, Negin, Qujeq, D., Yousefi, T., Soghli, Negar, 2020. The regulatory functions of circular RNAs in osteosarcoma. Genomics 112, 2845–2856. https://doi.org/10.1016/j.ygeno.2020.03.024

Su, M., Xiao, Y., Ma, J., Tang, Y., Tian, B., Zhang, Y., Li, X., Wu, Z., Yang, D., Zhou, Y., Wang, H., Liao, Q., Wang, W., 2019. Circular RNAs in Cancer: emerging functions in hallmarks, stemness, resistance and roles as potential biomarkers. Mol Cancer 18, 90. https://doi.org/10.1186/s12943-019-1002-6

Suzuki, H., Zuo, Y., Wang, J., Zhang, M.Q., Malhotra, A., Mayeda, A., 2006. Characterization of RNase R-digested cellular RNA source that consists of lariat and circular RNAs from pre-mRNA splicing. Nucleic Acids Res 34, e63. https://doi.org/10.1093/nar/gkl151

Vincent, H.A., Deutscher, M.P., 2006. Substrate recognition and catalysis by the exoribonuclease RNase R. J Biol Chem 281, 29769–29775. https://doi.org/10.1074/jbc.M606744200

Wang, J., Lin, Y., Jiang, D.-H., Yang, X., He, X.-G., 2021. CircRNA ZNF609 promotes angiogenesis in nasopharyngeal carcinoma by regulating miR-145/STMN1 axis. Kaohsiung J Med Sci 37, 686–698. https://doi.org/10.1002/kjm2.12381

Wang, S., Wu, J., Wang, Zhongyuan, Gong, Z., Liu, Y., Wang, Zengjun, 2022. Emerging Roles of Circ-ZNF609 in Multiple Human Diseases. Front Genet 13, 837343. https://doi.org/10.3389/fgene.2022.837343

Wang, S., Xue, X., Wang, R., Li, X., Li, Q., Wang, Y., Xie, P., Kang, Y., Meng, R., Feng, X., 2018. CircZNF609 promotes breast cancer cell growth, migration, and invasion by elevating p70S6K1 via sponging miR-145-5p. Cancer Manag Res 10, 3881–3890. https://doi.org/10.2147/CMAR.S174778

Wu, L., Xia, J., Yang, J., Shi, Y., Xia, H., Xiang, X., Yu, X., 2018. Circ-ZNF609 promotes migration of colorectal cancer by inhibiting Gli1 expression via microRNA-150. J BUON 23, 1343–1349.

Yang, X., Mei, J., Wang, H., Gu, D., Ding, J., Liu, C., 2020. The emerging roles of circular RNAs in ovarian cancer. Cancer Cell Int 20, 265. https://doi.org/10.1186/s12935-020-01367-9

Yoshikawa, H., Larance, M., Harney, D.J., Sundaramoorthy, R., Ly, T., Owen-Hughes, T., Lamond, A.I., 2018. Efficient analysis of mammalian polysomes in cells and tissues using Ribo Mega-SEC. Elife 7, e36530. https://doi.org/10.7554/eLife.36530

Zhang, Z., Wang, C., Zhang, Y., Yu, S., Zhao, G., Xu, J., 2020. CircDUSP16 promotes the tumorigenesis and invasion of gastric cancer by sponging miR-145-5p. Gastric Cancer 23, 437–448. https://doi.org/10.1007/s10120-019-01018-7